

Regionalization-based spatiotemporal variations of precipitation regimes across China

Mingzhong Xiao · Qiang Zhang · Vijay P. Singh · Xiaohong Chen

Received: 7 November 2012 / Accepted: 2 January 2013 / Published online: 17 January 2013
© Springer-Verlag Wien 2013

Abstract Daily precipitation data from 595 stations are analyzed based on regionalization to investigate changing properties of precipitation regimes across the entire China. The results indicate that the northwestern China is characterized by increasing monthly precipitation. The abrupt increase of precipitation is after early 1980s and early 1990s in the western arid zone and Qinghai-Tibet plateau, respectively. Other climate zones are dominated by decreasing precipitation regimes in autumn and increasing precipitation regimes in winter, and it is particularly true in the southwestern, southern and central China, showing seasonal shifts of precipitation changes. Besides, weak precipitation regimes are decreasing and strong precipitation regimes are increasing, and it is particularly the case in the southwestern, southern and central China, implying intensifying hydrological cycle reflected by precipitation changes in these regions. This study steps further into different hydrological responses within different regions of China to climate changes and will be relevant in regional management of agriculture development and water resources.

1 Introduction

Nowadays, increasing evidence tends to indicate intensified hydrological cycle due to changing climate (Bates et al. 2008) and human activities (Min et al. 2011), leading to more frequent and more intensive extreme hydrological phenomena, such as heavy precipitation and related floods and droughts (e.g., Groisman et al. 2005). Changes of floods and droughts are closely related to changing properties of precipitation extremes in both space and time. Moreover, increasing frequency and intensity of floods and droughts are the major natural hazards negatively influencing human society and causing great socioeconomic loss. Therefore, there are a bunch of researches pertaining to precipitation changes (Christensen and Christensen 2004; Dore 2005).

China is located in the East Asia (Fig. 1); one of the most destructive climate events in China is the extreme precipitation during the summer monsoon season. The summer monsoon rainfall brings a necessary water supply for growing crops to nourish more than one billion people. As such, variability and change in precipitation amounts and extreme precipitation are major concerns for both the Chinese government and the public. Numerous studies have documented the precipitation changes in China. Becker et al. (2004) related rainfall variability in the Yangtze basin to v-wind variability at the 700-hPa level over southern China. It is evident that the precipitation in the region not only depends on the monsoon intensity but also on the amount of water vapor that is transported by the system. Zhai et al. (2005) indicated moderate changes of total precipitation in China during 1951–2000 with distinct regional and seasonal patterns of trends. Wang and Zhou (2005) have studied the large-scale circulation trend associated with the trends in extreme events, and found that the summer circulation over East Asia showed a strengthening trend of the continental high over Eurasia and a weakening trend of the western Pacific subtropical high, resulting to the annual and summer

M. Xiao · Q. Zhang (✉) · X. Chen
Department of Water Resources and Environment, Sun Yat-sen University, Guangzhou 510275, China
e-mail: zhangq68@mail.sysu.edu.cn

M. Xiao · Q. Zhang · X. Chen
Key Laboratory of Water Cycle and Water Security in Southern China of Guangdong High Education Institute,
Sun Yat-sen University, Guangzhou 510275, China

M. Xiao · Q. Zhang · X. Chen
School of Geography and Planning, and Guangdong Key Laboratory for Urbanization and Geo-simulation, Sun Yat-sen University, Guangzhou, People's Republic of China

V. P. Singh
Department of Biological & Agricultural Engineering and
Department of Civil and Environmental Engineering,
Texas A & M University, College Station, TX 77843-2117, USA

mean precipitation, and the extreme precipitation events in summer consistently decreased in north China and increased in the middle-lower reaches of Yangtze River. And based on the daily precipitation time series of 590 rain stations in China covering 1960–2005 and the water vapor flux, Zhang et al. (2011a) found that there are tremendous influences of water vapor flux on the precipitation changes across China, regions east to 100 °E were dominated by increasing water vapor flux in winter.

In this study, based on updated daily precipitation dataset and the climatic regionalization of China (Zhang and Lin 1985), China was subdivided into eight climatic regions: western arid (semiarid) zone, Qinghai-Tibet plateau, eastern arid zone, southwestern, northeastern, northern, central, and southern China (Fig. 2). For each region, the temporal evolutions of the monthly precipitations within a year have been analyzed. Meanwhile, ten precipitation quantile indices have been defined in the study, and then, the temporal evolutions of the precipitation quantile indices anomalies in each region have been analyzed to show the spatiotemporal variations of precipitation regimes. This study can merit regional water resources management and also study of regional hydrological responses to climate changes. This is the major motivation of this current study.

Milly et al. (2008) argued that climate change undermines stationarity, a basic assumption that historically has assisted practice and research in the fields of hydrology and water resources management. And Silva et al. (2012) have made an exploratory analysis on the variability of flood occurrence rates in ten Portuguese watersheds. To analyze the variability of precipitation occurrence rates, the time-dependent occurrence rates of extreme precipitation for each region in China also have been conducted in the study. Besides, precipitation analysis based on regionalization will definitely be relevant in terms of regional water resources management and planning of development of agricultural activities. The paper is organized as follows. We describe the datasets in Section 2 and analysis methods in Section 3. Section 4 presents and discusses the results of the study, and, finally, in Section 5, the most relevant conclusions of the article are drawn.

2 Data

Daily precipitation, updated to December 31, 2009, from 595 meteorological stations across China was analyzed, and the locations of these gauging stations are shown in Fig. 1. The datasets were obtained from the National Climate Center of China Meteorological Administration. The lengths of time series of these gauging stations range from 36 to 59 years as shown in Fig. 1, and there are 148 gauging stations containing missing days (shown in Fig. 1). However, only one station had 1.54 % missing values, and

most of them had less than 0.1 % of total missing values. These series with missing values were replaced by the long-term average of the same days of other years. Based on the objectives of this study, the gap-filling method did not significantly affect the final results. The similar gap-fill method has also been used by Zhang et al. (2011b).

To analyze precipitation characteristics, several indices were considered in this study. The monthly total precipitation amounts of the wet days for each station have been studied, and the wet day was defined as the day with precipitation exceeding 1 mm. For each region, the regional monthly precipitations were the arithmetic average of the monthly precipitation of all the stations in the sub-regions. As the time series of daily precipitation in each station are not the same, in this study we only extracted the same time series of daily precipitation for each station in a sub-region to analyze the monthly precipitation, and then the monthly precipitation within a year. For comparison, the monthly precipitation anomalies within a year have been normalized using the standard normal distribution. Furthermore, we defined ten precipitation quantile indices by taking a year as the time scale based on the 90th, 80th, 70th, 60th, 50th, 40th, 30th, 20th, and 10th percentile thresholds, and the percentile thresholds were calculated based on the precipitation series of all wet days in the first 30-year periods at each station (Alexander et al. 2006; Table 1).

3 Methodologies

Occurrence rates are analyzed using the nonparametric occurrence rate estimation methods. The point process is specified as a stationarity Poisson process if it has constant occurrence rate λ . The unit of the occurrence rate λ is one over time units given the probability per time interval that an extreme occurs. For studying nonstationarity Poisson process, we now introduce time dependence and denote the function $\lambda(t)$ as occurrence rate (Mudelsee 2010).

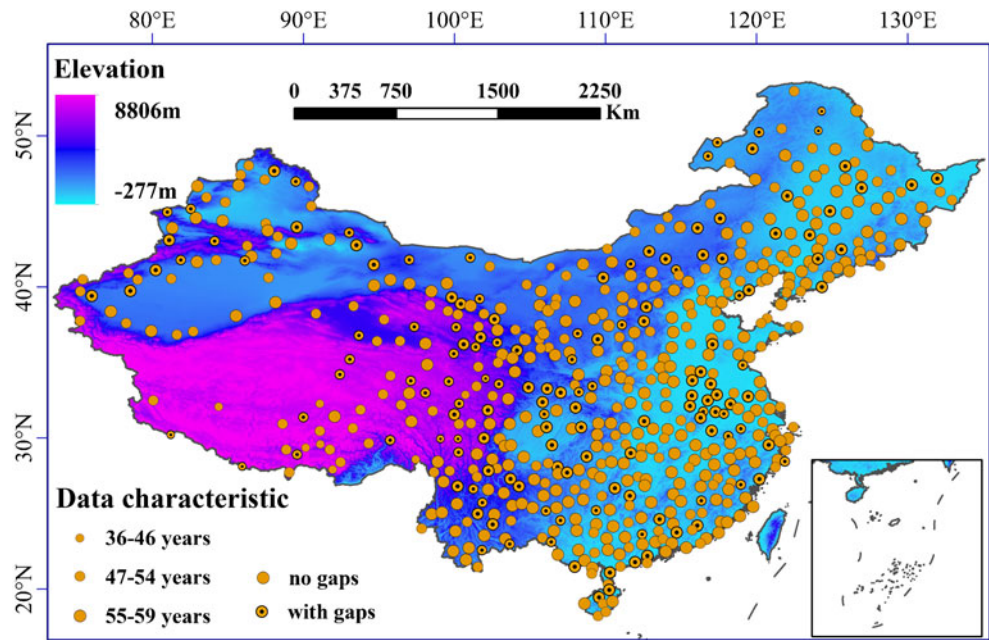
The Kernel technique is a nonparametric method developed by Diggle (1985) for smoothing point process data. For estimating the intensity of a point process such as the time-dependent occurrence rate, $\lambda(t)$, this technique can be formulated as:

$$\hat{\lambda}(t) = h^{-1} \sum_{i=1}^m K\left(\frac{t - \tau_i}{h}\right) \quad (1)$$

where K is the kernel function and h is the bandwidth. A Gaussian kernel was used as it can be efficiently calculated in Fourier space and yields a smooth estimated occurrence rate, $\hat{\lambda}(t)$ (Mudelsee et al. 2003; Mudelsee 2010):

$$K(y) = \frac{1}{\sqrt{2\pi}} \exp\left(-\frac{y^2}{2}\right) \quad (2)$$

Fig. 1 Location of the gauging stations in China and the characteristic of the daily precipitation in each station



The units of $\hat{\lambda}(t)$ are d^{-1} , i.e., the number of occurrences above threshold per day at a given point in time, t . However, to facilitate the interpretation of the results, $\hat{\lambda}(t)$ was multiplied by 365.25, such that, for a given instant, t , the $\hat{\lambda}(t)$ indicates the estimated number of occurrences above threshold per year.

The application of Eq. (1) may lead to a boundary bias near t_o and t_n consisting of an underestimation of $\lambda(t)$ due to the nonexistence of data outside the interval $[t_o, t_n]$. This boundary effect can be reduced by generating pseudodata, i.e., pseudo extreme events, pT , outside of the observation interval, before estimating $\lambda(t)$. The straightforward method of reflection was used to generate pseudodata (on the left side, for $t < t_o$: $pT(i) = t_o - [T_i - t_o]$, covering an amplitude of three times h before t_o ; analogously on the right side, for $t > t_n$). Pseudodata generation is equivalent to the extrapolation of the empirical distribution of events near the boundaries; hence, the estimation of $\lambda(t)$ near the boundaries of the observation period should be

analyzed with caution (Mudelsee 2010). Considering T^* as the original point data, T , augmented by the pseudodata, pT , and m^* as the total number of points in T^* , Eq. (1) can be rewritten as:

$$\hat{\lambda}(t) = h^{-1} \sum_{i=1}^{m^*} K\left(\frac{t - \tau_i}{h}\right) \tag{3}$$

The selection of the bandwidth, h , determines the bias and variance properties of the occurrence rate estimator $\hat{\lambda}(t)$: a too small h results in fewer data points that effectively contribute to the kernel estimation, which leads to a reduced bias and a high variance; on the other hand, a too large h leads to an oversmoothing of the estimator, resulting in a small variance and increased bias. The selection of the bandwidth can be seen as a compromise between those two cases. In this study, the selection of the bandwidth used the cross-validation bandwidth selector developed by Brooks and Marron (1991). This is the minimizer of (Mudelsee 2010):

$$c(h) = \int_{T_1}^{T_m} [\hat{\lambda}(T)]^2 dT - 2 \sum_{j=1}^m \hat{\lambda}_j(T_j) \tag{4}$$

where

$$\hat{\lambda}_j(T) = \sum_{k=1, k \neq j}^m h^{-1} K\left(\frac{T - T_k}{h}\right) \tag{5}$$

is the delete-one estimate. Furthermore, as the objective is to describe inter-annual variability of $\hat{\lambda}(t)$, the bandwidth should be considerably higher than the year to avoid the effect of the seasonal variability.

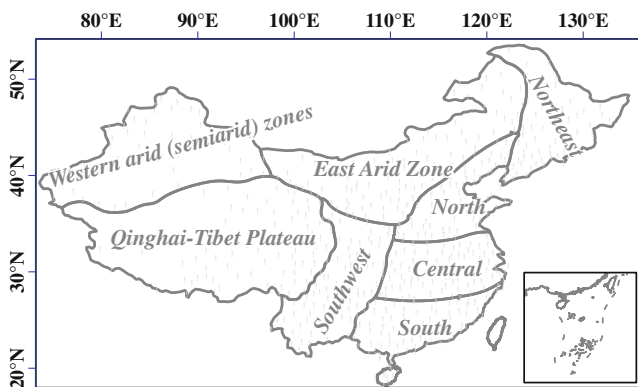


Fig. 2 Climatic regionalization of China with eight climate zones

Table 1 The definition of the ten quantile precipitation indices

Quantile precipitation indices	Definitions
Ex1	The total precipitation amounts of daily precipitation exceeding the 90th percentile threshold in a year
Ex2	The total precipitation amounts of daily precipitation exceeding the 80th percentile threshold while less than the 90th percentile threshold in a year
Ex3	The total precipitation amounts of daily precipitation exceeding the 70th percentile threshold while less than the 80th percentile threshold in a year
Ex4	The total precipitation amounts of daily precipitation exceeding the 60th percentile threshold while less than the 70th percentile threshold in a year
Ex5	The total precipitation amounts of daily precipitation exceeding the 50th percentile threshold while less than the 60th percentile threshold in a year
Ex6	The total precipitation amounts of daily precipitation exceeding the 40th percentile threshold while less than the 50th percentile threshold in a year
Ex7	The total precipitation amounts of daily precipitation exceeding the 30th percentile threshold while less than the 40th percentile threshold in a year
Ex8	The total precipitation amounts of daily precipitation exceeding the 20th percentile threshold while less than the 30th percentile threshold in a year
Ex9	The total precipitation amounts of daily precipitation exceeding the 10th percentile threshold while less than the 20th percentile threshold in a year
Ex10	The total precipitation amounts of daily precipitation exceeding 1mm while less than the 10th percentile threshold in a year

4 Results

4.1 Temporal evolutions of monthly precipitation

The temporal distribution of the regional average monthly precipitation (Fig. 3a) and precipitation quantile indices (Fig. 3b) in a year are illustrated in Fig. 3. It can be observed from Fig. 3a that precipitation mainly occurs during June, July, and August with peak precipitation value in July except southern China where the temporal distribution of monthly precipitation is characterized by two peak precipitation values in June and August. Besides, Fig. 3 also shows that the seasonal variability of precipitation regimes is larger from the northwest to the east and to the southeast China.

It can be seen from Fig. 4a, b that increase of precipitation has been observed during most of the months at western arid (semiarid) zone and which is consistent with the results by Zhai et al. (2005) and Zhang et al. (2011a, b; 2012a, b). Larger increasing magnitude of precipitation is detected in January, November, and December. Relatively smaller increasing magnitude of precipitation is found in September, July, and March. Temporal changes of monthly precipitation (left panel of Fig. 4a) indicate that mid-1980s can be taken as the transitional time when the northwestern China shifts from dry to wet climate status. Changing properties of precipitation in the Qinghai-Tibet plateau are different from those in the western arid zone. Evident increase of monthly precipitation is observed mainly from January to May. Decreasing precipitation is identified in June and December, respectively. Besides, the

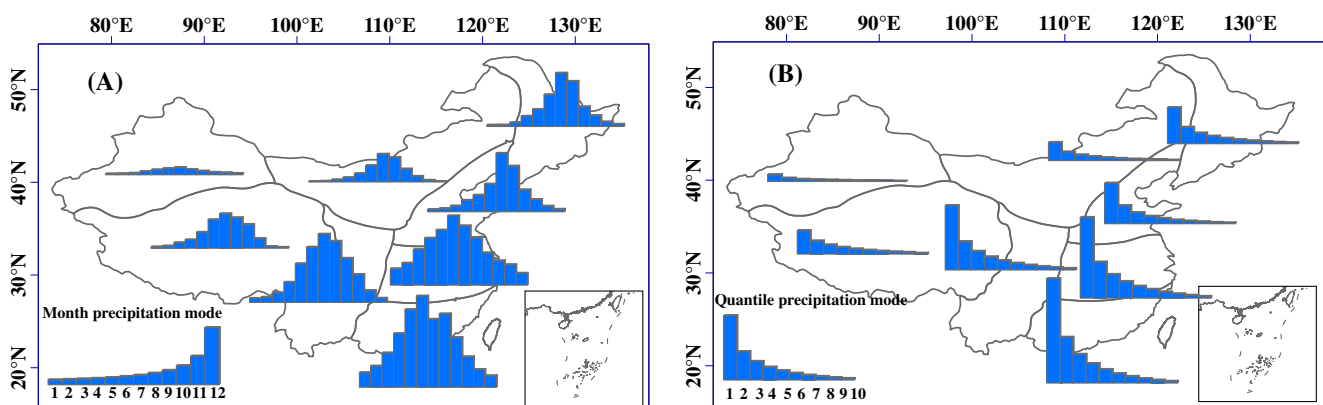


Fig. 3 The regional annual monthly precipitation (a) and the regional annual precipitation quantile indices for all of the climate regions (b) over China

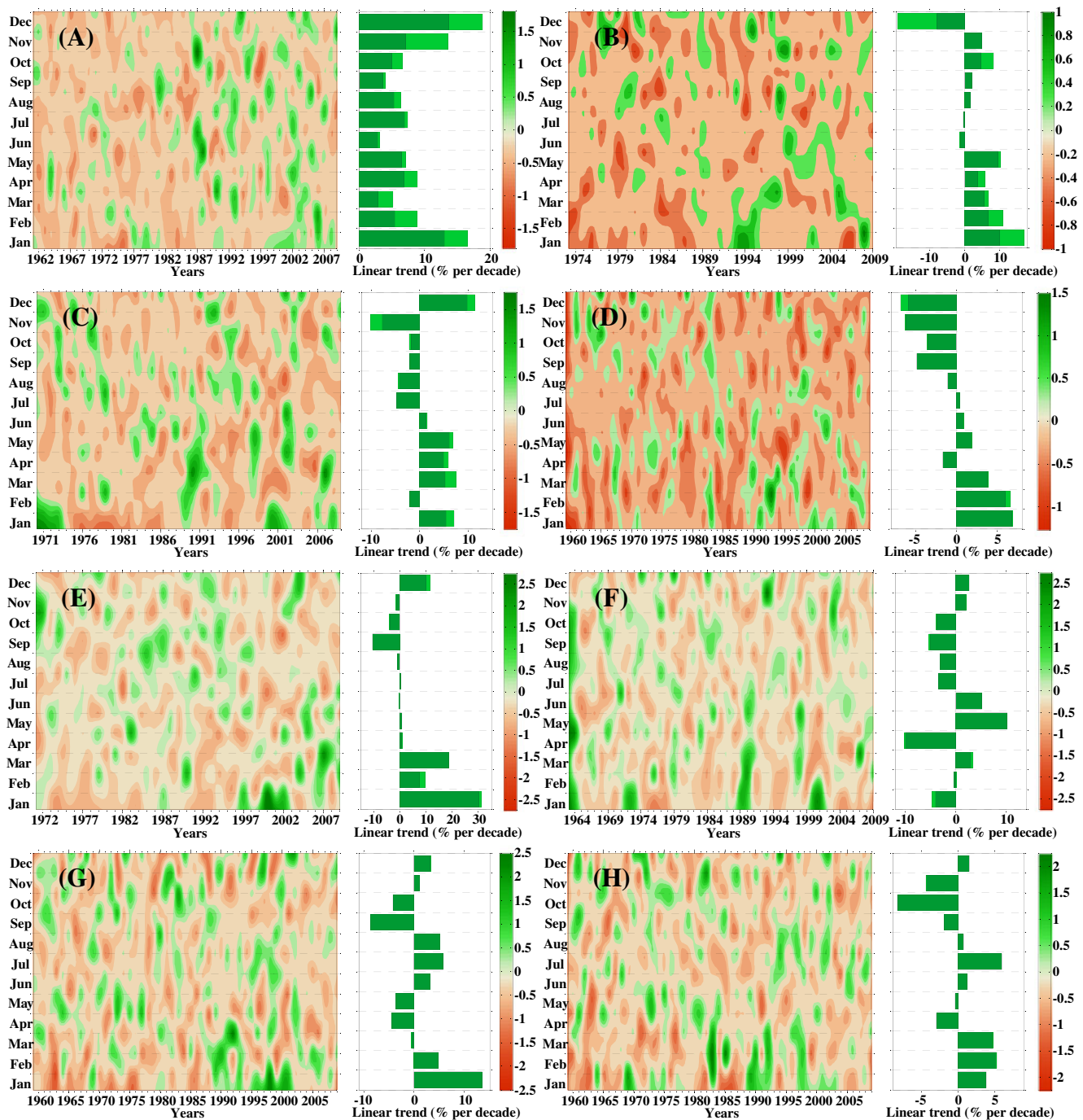


Fig. 4 Temporal evolution of the normalized monthly precipitation anomalies in a year and the linear trends (percentage per decade) of the monthly precipitation (green bars) along with their 95 % significance (dark shaded bars) for Western arid (semiarid) zone (a), for Qinghai-

Tibet plateau (b), for East arid zone (c), for Southwest China (d), for Northeast China (e), for North China (f), for Central China (g), and for South China (h). Specific regions can be referred to Fig. 2

increasing magnitude in general in the Qinghai-Tibet plateau is also smaller than that in the western arid zone. The left panel of Fig. 4b shows no clear changing patterns of monthly precipitation. However, increasing precipitation seems to concentrate in spring and parts of the months of winter in recent years and specifically after early 1990s.

Precipitation changes in the eastern arid zone (Fig. 4c), southwestern China (Fig. 4d), and northeastern China (Fig. 4e) are similar. Decreasing precipitation is observed mainly from August to December and increasing precipitation from January to June. Left panel of Fig. 4c shows that increasing precipitation is observed mainly during the time

interval from July to December, and shifts to the time interval from January to May after early 1990s. Similar characteristics are also found in the temporal changes of precipitation as shown in the left panel of Fig. 4d, e. Changes of monthly precipitation in other three regions, i.e., northern China (Fig. 4f), central China (Fig. 4g), and

southern China (Fig. 4h), are relatively complicated, and no fixed patterns can be identified. Summer precipitation (June, July, and August) is subject to smaller changing magnitude and even decrease. These results are in good agreement with those by Wang and Zhou (2005) that as the result of the summer circulation over East Asia showing a strengthening

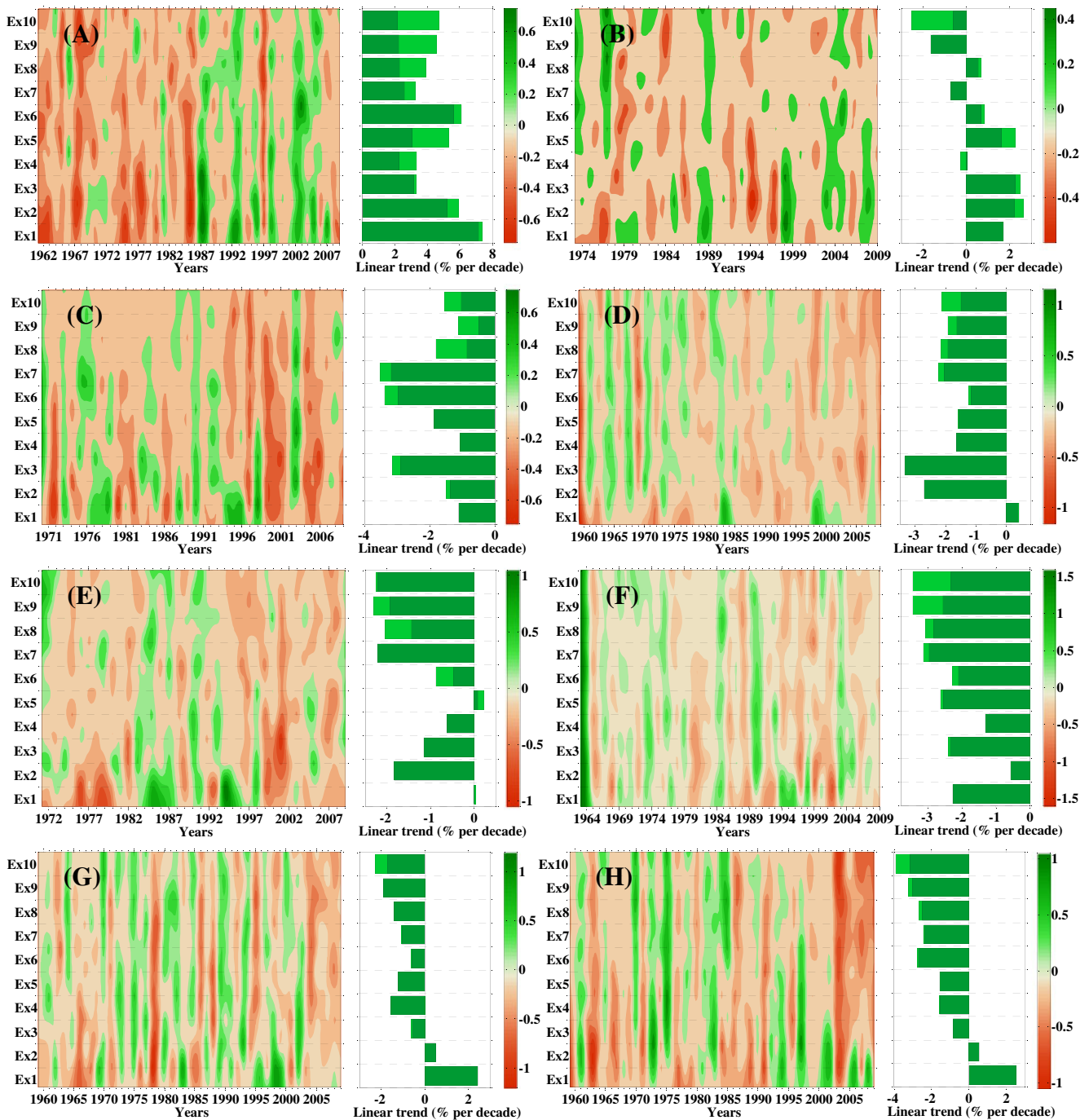


Fig. 5 Temporal evolution of the normalized precipitation quantile indices anomalies in a year and the linear trends (percentage per decade) of the precipitation quantile indices (*green bars*) along with their 95 % significance (*dark shaded bars*) for Western arid (semiarid)

zone (a), for Qinghai-Tibet plateau (b), for East arid zone (c), for Southwest China (d), for Northeast China (e), for North China (f), for Central China (g), and for South China (h). The specific locations of these zones can be referred to Fig. 2

trend of the continental high over Eurasia and a weakening trend of the western Pacific subtropical high, the annual and summer mean precipitation and the extreme precipitation events in summer consistently decreased in northern China and increased in the middle and lower reaches of the Yangtze River basin.

4.2 Temporal evolutions of precipitation quantile indices

Figure 5 illustrates temporal changes of precipitation regimes defined by percentiles. Ex1 denotes strong precipitation process, and other indices such as Ex2 to Ex10 denote weak precipitation processes. Distinct changing features of precipitation extremes can be identified in Fig. 5. Precipitation

regimes are subject to similar changing properties in western arid zone and Qinghai-Tibet plateau (Figs. 5a, b). Strong precipitation regimes, i.e., Ex1, are increasing and increasing weak precipitation regimes are also dominant. However, the Ex10, Ex9, Ex7, and Ex4 are decreasing with different changing magnitude (Fig. 5b). Increasing precipitation regimes occur mainly after mid-1980s and which is in good line with that of monthly precipitation (Fig. 5a). Evident increase of Ex1–Ex5 starts after roughly 1999 (Fig. 5b).

Precipitation regimes in the eastern arid zone (Fig. 5c), the northeastern China (Fig. 5e), and the northern China (Fig. 5f) are in similar changes. Both strong and weak precipitation regimes are decreasing, and the decrease occurred after early-1990s. However, different changing properties of precipitation

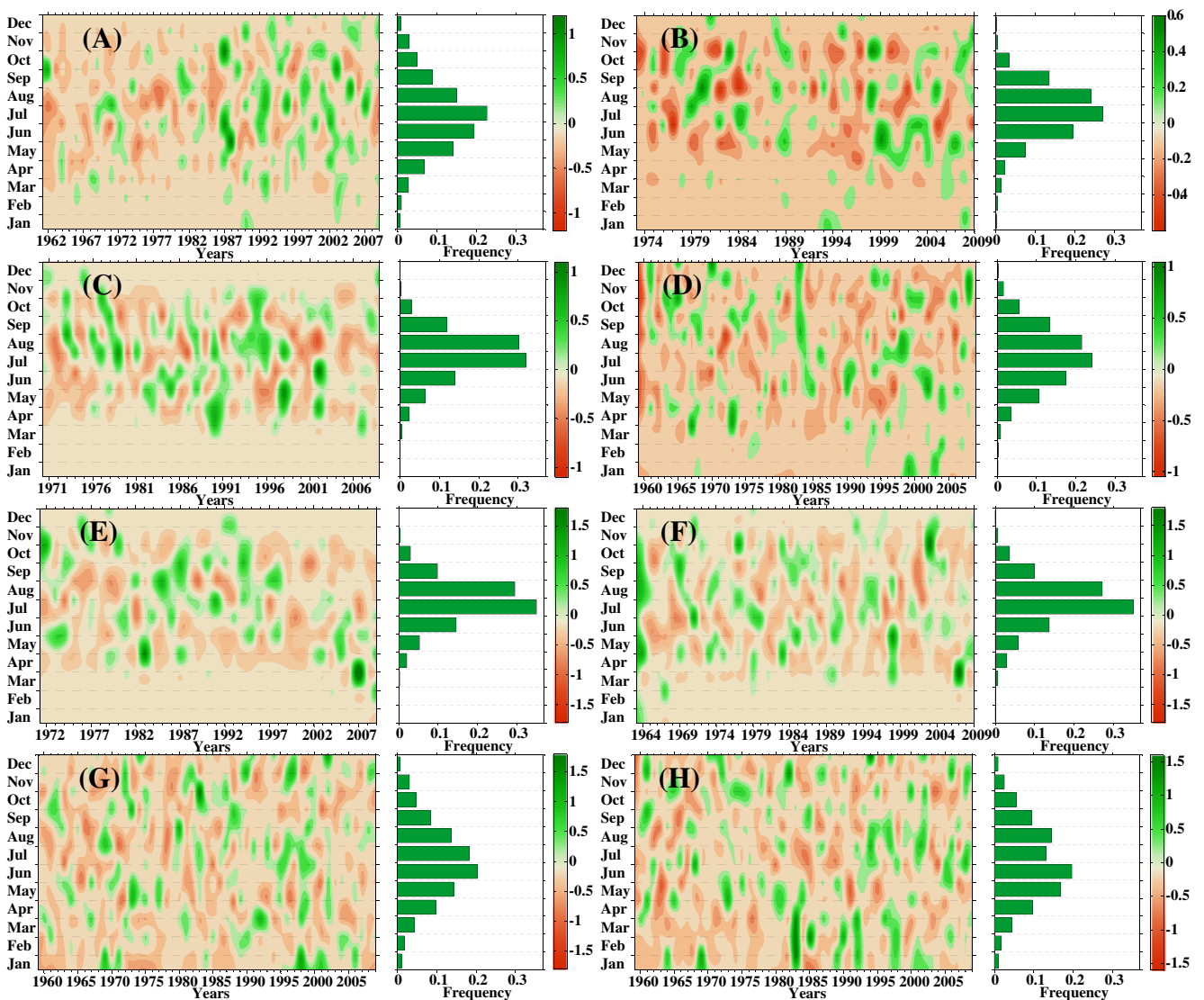


Fig. 6 Temporal evolution of the normalized occurrence frequency anomalies of 90 % extreme precipitation events in a year and the linear trends (percentage per decade) of the occurrence frequency of 90 % extreme precipitation events (green bars) along with their 95 %

significance (dark shaded bars), a for Western arid (semiarid) zone, b for Qinghai-Tibet plateau, c for East arid zone, d for Southwest China, e for Northeast China, f for North China, g for Central China, and h for South China, referring to Fig. 2

regimes can be detected in southwestern China (Fig. 5d), central China (G), and southern China (H). Precipitation regimes in these three regions are dominated by decreasing weak precipitation regimes but increasing strong precipitation regimes. The time when abrupt changes of weak and strong precipitation regimes occurred is roughly in early 1990s.

4.3 Temporal changes of occurrence of 90 % precipitation extremes

The 90 % extreme precipitation events are defined as daily precipitation exceeding the 90th percentile threshold, and the occurrence frequency of 90 % extreme precipitation

events in each month for each sub-region has been illustrated in Fig. 6. It can be observed from Fig. 6 that different changing properties of frequency of 90 % precipitation extremes can be identified in different regions. Generally, Fig. 6a, b demonstrates similar changing features, i.e., 90 % precipitation extremes occur mainly during June and July. Similar changing properties of 90 % precipitation extremes can be observed in southwestern China (Fig. 6d), central China (Fig. 6g), and southern China (Fig. 6h). Meanwhile, evident increase of occurrence of 90 % precipitation extremes can be identified after early 1980s in the western arid (semiarid) zone and less obvious increase in July and August in the central and southern China (Fig. 6g, h).

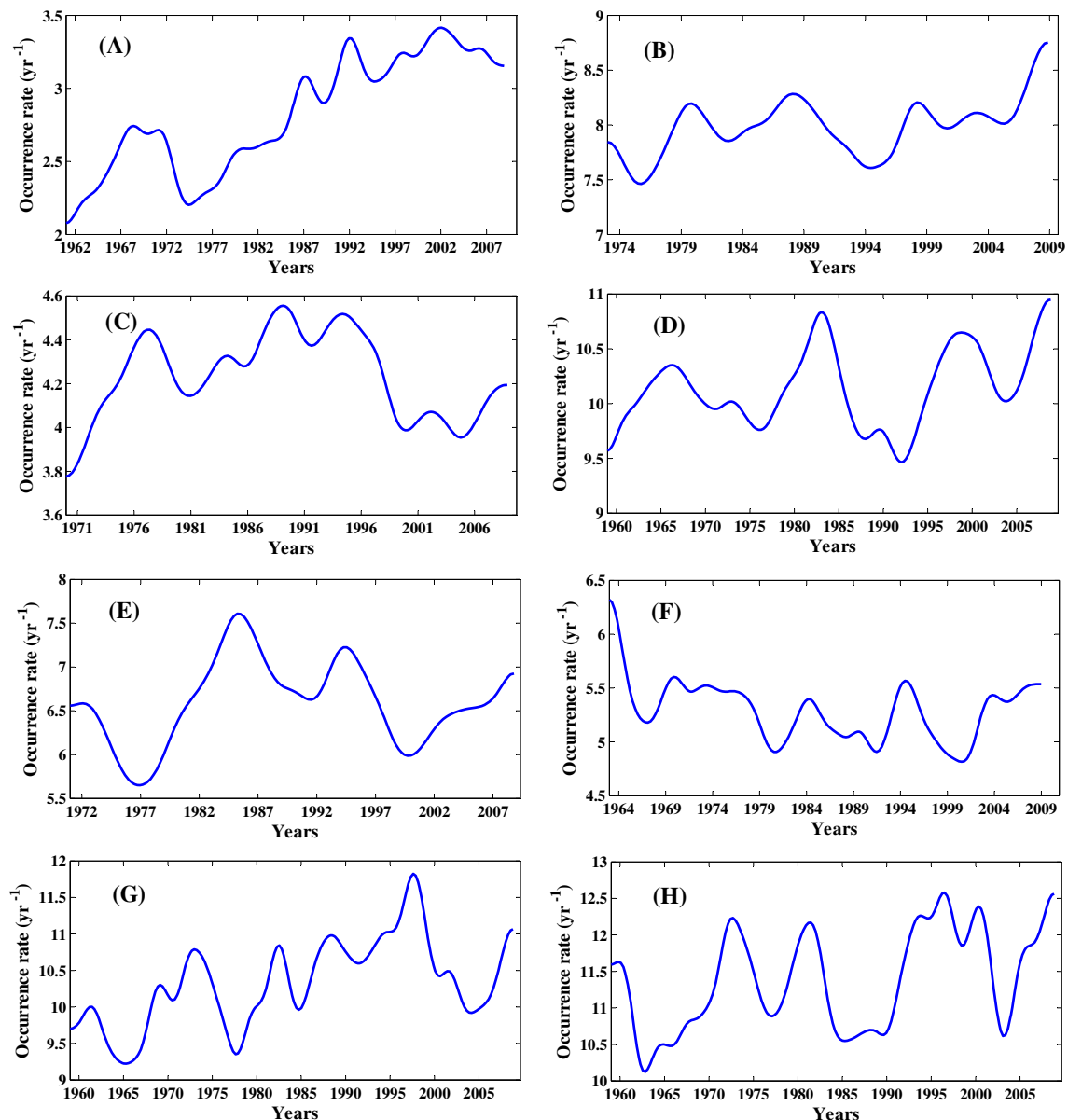


Fig. 7 Estimated occurrence rates for 90 % extreme precipitation events: **a** for Western arid (semiarid) zone, **b** for Qinghai-Tibet plateau, **c** for East arid zone, **d** for Southwest China, **e** for Northeast China, **f** for North China, **g** for Central China, and **h** for South China, referring to Fig. 2

Occurrence of 90 % precipitation extremes in the east arid zone (Fig. 6c), the northeastern China (Fig. 6e), and the northern China (Fig. 6f) is significantly concentrated during July and August, and particularly in July. Furthermore, it can be seen from Fig. 6c, e that for east arid zone and northeast China, the 90 % extreme precipitation events tend to occur earlier.

Based on the previous results illustrated in Section 4.1, the trend of the 90 % extreme precipitation events in each month for each sub-region is consistent with those of Fig. 4, meaning that the alterations of month precipitation are mainly caused by the alterations of extreme precipitation in that month, especially for the western arid (semiarid) zone, eastern arid zone, northeastern, central and southern China.

4.4 Occurrence rate of 90 % extreme precipitation

Figure 7 shows the regional average occurrence rate of 90 % extreme precipitation events. Evident increase of 90 % extreme precipitation can be found in the western arid (semiarid) zone (Fig. 7a) after early 1980s, and it is similar with those by monthly precipitation and precipitation quantile indices. Increase of 90 % extreme precipitation can also be observed in mid-1990s in the Qinghai-Tibet plateau (Fig. 7b). A slight decrease of 90 % extreme precipitation is identified in the eastern arid zone (Fig. 7c), northeastern China (Fig. 7e), and in northern China (Fig. 7f). The decrease in the Qinghai-Tibet plateau (Fig. 7c) and in the northeastern China (Fig. 7e) is after mid-1980s. However, the general decrease of 90 % extreme precipitation is identified in northern China (Fig. 7f) throughout the entire study time interval. The 90 % extreme precipitation in southwestern China (Fig. 7d), central China (Fig. 7g), and in southern China (Fig. 7h) is in moderate changes without evident increase or decrease, showing different patterns of precipitation extremes.

5 Brief discussions and conclusions

Spatial and temporal distribution of precipitation regimes is relevant in terms of understanding of regional responses of hydrological cycle, such as the precipitation changes in this study, to climate changes and also in regional planning of agriculture development and regional water resources management. Based on regionalization, changes of the regional precipitation regimes are analyzed.

Different changing properties are identified for different regions based on regionalization over China. In general, similar changing features of precipitation regimes can be found in three groups of regions or climate zones, i.e., the western arid (semiarid) zone and Qinghai-Tibet plateau zone; the eastern arid zone, northeastern China and northern

China; and southeastern China, the central China, and southern China. And these three groups of regions are actually three climate zones covering larger geographical area. Based on analysis results of reference evapotranspiration over China (Zhang et al. 2011c), these three climate zones are roughly corresponding to the regions covered by different reference evapotranspiration changes, showing different hydrological responses within China to climate changes reflected by precipitation and reference evapotranspiration.

Increasing precipitation is observed mainly in the western arid (semiarid) and Qinghai-Tibet plateau zones. In other regions, particularly in the central and southern China, decreasing precipitation occurs in autumn and increasing precipitation in winter. This result mirrors seasonal shifts of precipitation variations and which was well corroborated by observed precipitation changes (Zhang et al. 2011a, b). Besides, weak precipitation regimes are decreasing and strong precipitation regimes are increasing, except for two regions, i.e., the western arid (semiarid) and Qinghai-Tibet plateau zones. These results tend to evidence intensification of hydrological cycle in China, particularly in the center and south China. Moreover, the results of this study also indicate higher intensification of hydrological cycle in the southwestern China when compared to other regions of China. This spatial pattern of precipitation changes will mean much for regional management of water resources and agricultural development and will be helpful for scientific understanding of different hydrological responses to climate changes.

Acknowledgments This work was financially supported by Xinjiang Technology Program (grant nos. 201001066-3 and 200931105), the National Natural Science Foundation of China (grant nos. 41071020 and 50839005), Program for New Century Excellent Talents in University and by the Geographical Modeling and Geocomputation Program under the Focused Investment Scheme (1902042) of The Chinese University of Hong Kong. Our cordial gratitude should be extended to critical comments and pertinent suggestions from anonymous reviewers and the editor, Prof. Dr. Hartmut Grassl, which are greatly helpful in further improvement of this manuscript.

References

- Alexander L, Zhang X, Peterson T, Caesar J, Gleason B, Klein Tank A, Haylock M, Collins D, Trewin B, Rahimzadeh F (2006) Global observed changes in daily climate extremes of temperature and precipitation. *J Geophys Res* 111(D05109):22
- Bates B, Kundzewicz ZW, Wu S, Palutikof J (2008) Climate change and water. Intergovernmental Panel on Climate Change (IPCC), Geneva
- Becker S, Gemmer M, King L, Jiang T (2004) Climate change in China and its contribution to Yangtze River floods. In: Jiang T, King L, Gemmer M, Kundzewicz ZW (eds) Climate change and Yangtze floods. Science Press, Beijing, pp 2-15
- Brooks MM, Marron JS (1991) Asymptotic optimality of the least-squares cross-validation bandwidth for kernel estimates of intensity functions. *Stochastic Processes and their Applications* 38(1):157-165

- Christensen O, Christensen J (2004) Intensification of extreme European summer precipitation in a warmer climate. *Glob Planet Chang* 44 (1):107–117
- Diggle, P., 1985. A kernel method for smoothing point process data. *Applied Statistics*, 138–147
- Dore HIM (2005) Climate change and changes in global precipitation patterns: what do we know? *Environ Int* 31:1167–1181
- Groisman PY, Richard WK, David RE, Thomas RK, Gabriele CH, Vyacheslav NR (2005) Trends in intense precipitation in the climate record. *J Climate* 18:1326–1350
- Milly P, Julio B, Malin F, Robert M, Zbigniew W, Dennis P, Ronald J (2008) Stationarity is dead science. *American Association for the Advancement of Science* 319:573–574
- Min S-K, Zhang X, Zwiers WF, Hegerl CG (2011) Human contribution to more-intense precipitation extremes. *Nature* 470:378–381
- Mudelsee M (2010) *Climate time series analysis: classical statistical and bootstrap methods*. Springer, New York
- Mudelsee M, Börngen M, Tetzlaff G, Grünwald U (2003) No upward trends in the occurrence of extreme floods in central Europe. *Nature* 425(6953):166–169
- Silva A, Portela M, Naghettini M (2012) Nonstationarities in the occurrence rates of flood events in Portuguese watersheds. *Hydrology and Earth System Sciences* 16(1):241–254
- Wang Y, Zhou L (2005) Observed trends in extreme precipitation events in China during 1961–2001 and the associated changes in large-scale circulation. *Geophys Res Lett* 32(9):L09707
- Zhai P, Zhang X, Wan H, Pan X (2005) Trends in total precipitation and frequency of daily precipitation extremes over China. *J Clim* 18(7):1096–1108
- Zhang J, Lin Z (1985) *Climate in China*. Shanghai Scientific and Technical Publishers, Shanghai (in Chinese)
- Zhang Q, Xu C-Y, Chen XH, Zhang ZX (2011a) Statistical behaviors of precipitation regimes in China and their links with atmospheric circulation 1960–2005. *Int J Climatol*. doi:10.1002/joc.2193
- Zhang Q, Singh VP, Li JF, Chen XH (2011b) Analysis of the periods of maximum consecutive wet days in China. *J Geophys Res* 116. doi:10.1029/2011JD016088, D23106
- Zhang Q, Xu C-Y, Chen XH (2011c) Reference evapotranspiration changes in China: natural processes or human influences? *Theor Appl Climatol* 103:479–488
- Zhang Q, Singh VP, Li J, Jiang F, Bai Y (2012a) Spatio-temporal variations of precipitation extremes in Xinjiang, China. *J Hydrol* 434–435:7–18
- Zhang Q, Li J, Singh VP, Xu C-Y, Bai Y (2012b) Changing structure of the precipitation process during 1960–2005 in the Xinjiang, China. *Theor Appl Climatol* 110(1–2):229–244